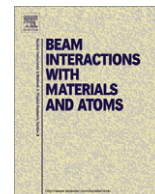




Contents lists available at ScienceDirect

## Nuclear Instruments and Methods in Physics Research B

journal homepage: [www.elsevier.com/locate/nimb](http://www.elsevier.com/locate/nimb)Sputtered neutral  $\text{Si}_n\text{C}_m$  clusters as a monitor for carbon implantation during  $\text{C}_{60}$  bombardment of siliconA. Wucher<sup>a,\*</sup>, A. Kucher<sup>b</sup>, N. Winograd<sup>b</sup>, C.A. Briner<sup>c</sup>, K.D. Krantzman<sup>c</sup><sup>a</sup> Fakultät für Physik, Universität Duisburg-Essen, 47048 Duisburg, Germany<sup>b</sup> Department of Chemistry, Pennsylvania State University, University Park, PA 16802, USA<sup>c</sup> Department of Chemistry and Biochemistry, College of Charleston, Charleston, SC 29424, USA

## ARTICLE INFO

## Article history:

Received 24 October 2010

Received in revised form 17 December 2010

Available online xxxx

## Keywords:

Sputtering

Cluster emission

Ion-surface interaction

Collision

Silicon

Carbon

Clusters

 $\text{C}_{60}$  bombardment

carbon implantation

## ABSTRACT

The incorporation of carbon atoms into a silicon surface under bombardment with 40-keV  $\text{C}_{60}^+$  ions is investigated using time-of-flight mass spectrometry of sputtered neutral and ionized  $\text{Si}_n\text{C}_m$  clusters. The neutral particles emitted from the surface are post-ionized by strong field infrared photoionization using a femtosecond laser system operated at a wavelength of 1400/1700 nm. From the comparison of secondary ion and neutral spectra, it is found that the secondary ion signals do not reflect the true partial sputter yields of the emitted clusters. The measured yield distribution is interpreted in terms of the accumulating carbon surface concentration with increasing  $\text{C}_{60}$  fluence. The experimental results are compared with those from recent molecular dynamics simulations of  $\text{C}_{60}$  bombardment of silicon.

© 2011 Elsevier B.V. All rights reserved.

## 1. Introduction

The bombardment of silicon with energetic  $\text{C}_{60}^+$  cluster ions leads to the incorporation of carbon into the Si target [1]. As a consequence,  $\text{Si}_n\text{C}_m$  clusters of varying sizes and compositions are found among the flux of particles sputtered from the surface. In principle, one would expect the distribution of  $n$  and  $m$  to be related to the chemical surface composition, which in turn evolves with accumulating projectile ion fluence until eventually a steady state is reached.

In a recently published study, Lyon and coworkers investigated the yield distribution of  $\text{Si}_n\text{C}_m^+$  secondary cluster ions as a function of  $\text{C}_{60}^+$  fluence [2]. The results were explained in terms of recent single-impact molecular dynamics (MD) simulations of  $\text{C}_{60}$  bombardment of silicon [3], which showed that C atoms are incorporated into the substrate by forming strong covalent bonds with Si atoms. The relative chemical composition of the measured  $\text{Si}_n\text{C}_m^+$  clusters was interpreted to reflect the original bonding configuration of the atoms in the substrate.

An important question that remained unexplored in this work is to which extent the measured secondary ion yields reflect the true composition of the sputtered material. It is well known that – at

least for clean metal and semiconductor surfaces – the majority of the sputtered particles are emitted as neutrals. Moreover, it has been established that ionization probabilities of sputtered clusters may strongly depend on the cluster size [4–8]. Since the MD simulations cannot predict the ionization state of the emitted particles, the results of such calculations must therefore in principle be compared to the yield distribution of sputtered neutral clusters rather than secondary ions.

In the present work, we use a high-intensity infrared laser photoionization scheme in order to detect the sputtered neutral  $\text{Si}_n\text{C}_m$  clusters emitted from a silicon surface under bombardment with energetic  $\text{C}_{60}^+$  cluster ions. The resulting yields of post-ionized neutrals are compared to those measured for the corresponding secondary ions. The secondary ion yield distributions exhibit a qualitatively different trend than those measured for the neutral clusters, manifesting that both data are needed in order to gain information regarding the true partial cluster yields. The resulting cluster yield distributions are compared to the results of recent MD simulations of multi-impact  $\text{C}_{60}$  bombardment of Si that model the effects of accumulating  $\text{C}_{60}$  fluence onto a silicon surface [9].

## 2. Experiment and simulations

The experiments were performed using a TOF-SIMS instrument described in detail elsewhere [10]. The system is equipped with a

\* Corresponding author. Tel.: +49 203 3792228; fax: +49 203 3792289.

E-mail address: [andreas.wucher@uni-due.de](mailto:andreas.wucher@uni-due.de) (A. Wucher).

high-intensity femtosecond laser system delivering approximately 0.4 mJ of energy into a pulse of 120 fs duration at a wavelength of 1450 and 1785 nm<sup>1</sup> and a repetition rate of 1 kHz. The idea behind this experiment is to operate in the strong field ionization regime in order to minimize photofragmentation during the post-ionization process. The infrared wavelength was chosen since it was recently found to ensure a softer but more efficient photoionization of sputtered molecules than the previously employed UV scheme [11]. It should be noted that previous experiments performed on sputtered germanium clusters using the same laser system as used here (although operated at a different wavelength of 266 nm) revealed photoionization characteristics comparable to VUV single photon ionization [12], which confirms our confidence that optimized “soft” photoionization conditions are employed in these experiments.

The laser beam was focused to a spot size of about 200  $\mu\text{m}$  diameter, thus yielding a peak power density of about  $1.5 \times 10^{13}$  W/cm<sup>2</sup>. This corresponds to a Keldysh non-adiabaticity parameter of the order of 1, indicating that we are indeed working in the field ionization regime. In order to get a feeling for the photoionization efficiency of the sputtered atoms, we employ Ammonov-Delone-Krainov (ADK) theory [13], using the respective ionization potential (8.15 and 12.22 eV for Si and C, respectively) as input parameters. The resulting post-ionization probabilities are  $5.8 \times 10^{-2}$  (Si) and  $1.7 \times 10^{-6}$  (C). In order to judge the reliability of these values, we divide the measured Si<sup>0</sup> signal by the calculated post-ionization probability and determine the Si<sup>+</sup> secondary ion formation probability  $\alpha_{\text{Si}^+}^+$  as the ratio between the measured Si<sup>+</sup> and the corrected Si<sup>0</sup> signals. As a result, we find  $\alpha_{\text{Si}^+}^+ \approx 1 \times 10^{-2}$  which is in good agreement with a value of  $8 \times 10^{-3}$  determined by Benninghoven and coworkers [14] for a clean silicon surface. For the sputtered clusters, we assume the photoionization process to be saturated, in accordance with our previous data on sputtered Ge<sub>n</sub> clusters [12].

The projectile ions were produced using a 40-keV C<sub>60</sub><sup>+</sup> source delivering a mass selected and focused beam of about 35 pA current and 10  $\mu\text{m}$  diameter impinging onto the surface under 40° with respect to the surface normal. The source was operated in a pulsed mode with about 2  $\mu\text{s}$  pulse duration. TOF mass spectra were acquired using a delayed extraction scheme, where the sample is kept at ground potential during the primary ion pulse and the extraction field is switched on at a delay of about 50 ns after the end of the ion pulse. This way, secondary ions are detected which reside above the surface at the switching time of the extraction field. Since the alignment of the TOF spectrometer was optimized for time focusing of photoions produced by the post-ionization laser, this leads to the detection of those secondary ions which are present in (or around) the post-ionization volume. The laser pulse is fired at a carefully selected delay time after switching the extraction field. This results in a temporal shift of secondary ion and post-ionized neutral peaks in the TOF spectrum, thus allowing to unambiguously separate between the two types of species. This is illustrated in Fig. 1, which shows a small portion of the measured TOF spectrum centered around the  $m/z$  28 Si peak. It is seen that secondary ion and neutral spectra could be acquired simultaneously, thereby avoiding the ambiguity introduced by sequential data acquisition cycles with laser and projectile ion beam being alternatively switched off and on. Moreover, peaks arising from photoionization of residual gas species were determined as a laser-only background spectrum and subtracted from those of post-ionized sputtered neutrals. While this strategy worked nicely for Si atoms and all Si<sub>n</sub> and Si<sub>n</sub>C<sub>m</sub> clusters, it was not possible to detect sputtered neutral carbon atoms and bare

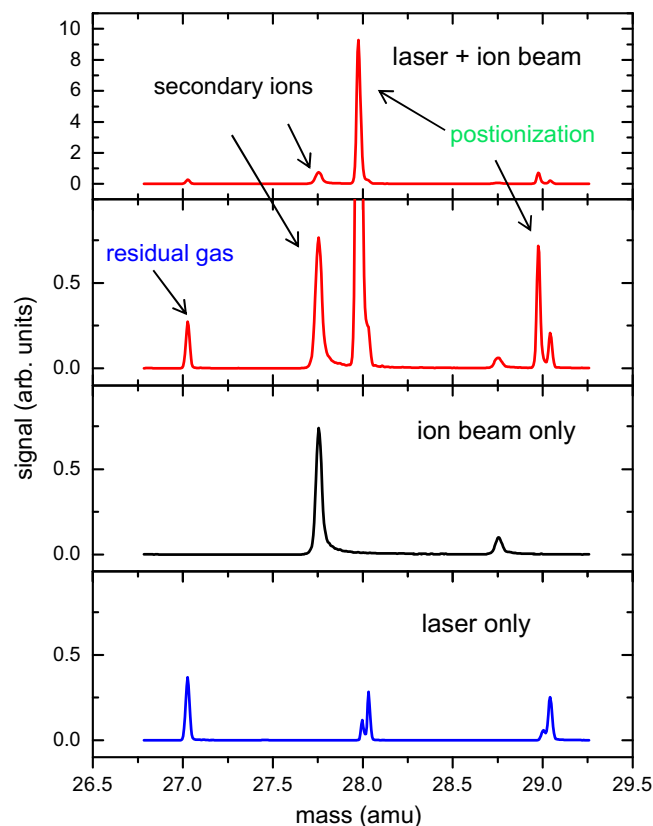


Fig. 1. TOF spectrum recorded around  $m/z$  28 illustrating the separation of the signals arising from post-ionized sputtered neutral particles, secondary ions and photoionized residual gas species.

C<sub>m</sub> clusters since the respective signals were masked by too large residual gas background.

The experiments were started on a fresh Si(1 0 0) surface which had not been bombarded before and therefore exhibited significant surface contamination (see below). Mass spectra were taken in a static mode, with a total ion fluence of about  $10^{11}$  ions/cm<sup>2</sup>, which is low enough that no part of the surface is influenced by more than a single impact. In order to investigate the effect of accumulating projectile fluence, the surface was then subjected to repeated bombardment cycles, where the primary ion beam was operated in a dc mode and rastered across an area of  $400 \times 400$  or  $100 \times 100 \mu\text{m}^2$ . The fluence applied during one of these cycles was  $1.2 \times 10^{13}$  and  $2.2 \times 10^{14}$  cm<sup>-2</sup>, respectively. Between successive sputtering cycles, mass spectra were again recorded from the central quarter of the sputtered area.

The MD simulations were performed with successive impacts of 20-keV C<sub>60</sub> impinging at normal incidence onto a reconstructed Si(1 0 0) surface. A “divide and conquer” scheme developed by Russo et al. [15] was used in order to treat multiple impacts of the bombarding projectile onto a single surface. Briefly, the surface is successively bombarded with the projectile directed to a set of impact points chosen randomly over the entire surface of a large master crystal, and the trajectory for each impact point is run using a smaller cylindrical sample extracted from the master crystal and then reinserted after the trajectory is complete. The model system is constructed of 66 layers of 7774 Si atoms and has dimensions of  $24 \times 24 \times 16$  nm. The top layer of Si atoms is reconstructed into dimers according to the well-known (2 × 1) structure. The surface is then equilibrated at 0 K using an algorithm based on the generalized langevin equation. A set of 200 impacts was simulated with impact points randomly chosen over the entire surface, which corresponds to a fluence of  $3.5 \times 10^{13}$  impacts/cm<sup>2</sup>. For each

<sup>1</sup> Both the signal and idler waves generated by an optical parametric amplifier were used in these experiments.

impact, a cylindrical volume of 8.3 nm radius and a 10 nm depth centered on the impact point was extracted from the master crystal. The MD trajectory was then run on that subsample, which was chosen to be large enough to include all atoms affected by the single impact. After completion of the single impact trajectory, the (now altered) volume was equilibrated at 0 K again and inserted back into the master crystal. An empirical many body potential developed by Tersoff [16] was used to model the Si–Si, Si–C and C–C interactions. A more detailed description of the simulations is given elsewhere [9].

### 3. Results

The measured signal intensity, i.e., the TOF signal integrated over the respective flight time peak, of sputtered neutral and ionized  $\text{Si}_n$ ,  $\text{Si}_n\text{C}$ ,  $\text{Si}_n\text{C}_2$  and  $\text{Si}_n\text{C}_3$  clusters are shown in Fig. 2. As already stated above, the first spectrum taken at zero fluence is strongly distorted by an organic surface contamination, which is apparently removed after the first sputtering cycle. Particularly for those clusters containing the most carbon atoms, this leads to very high intensities in the first mass spectrum, which then quickly decay

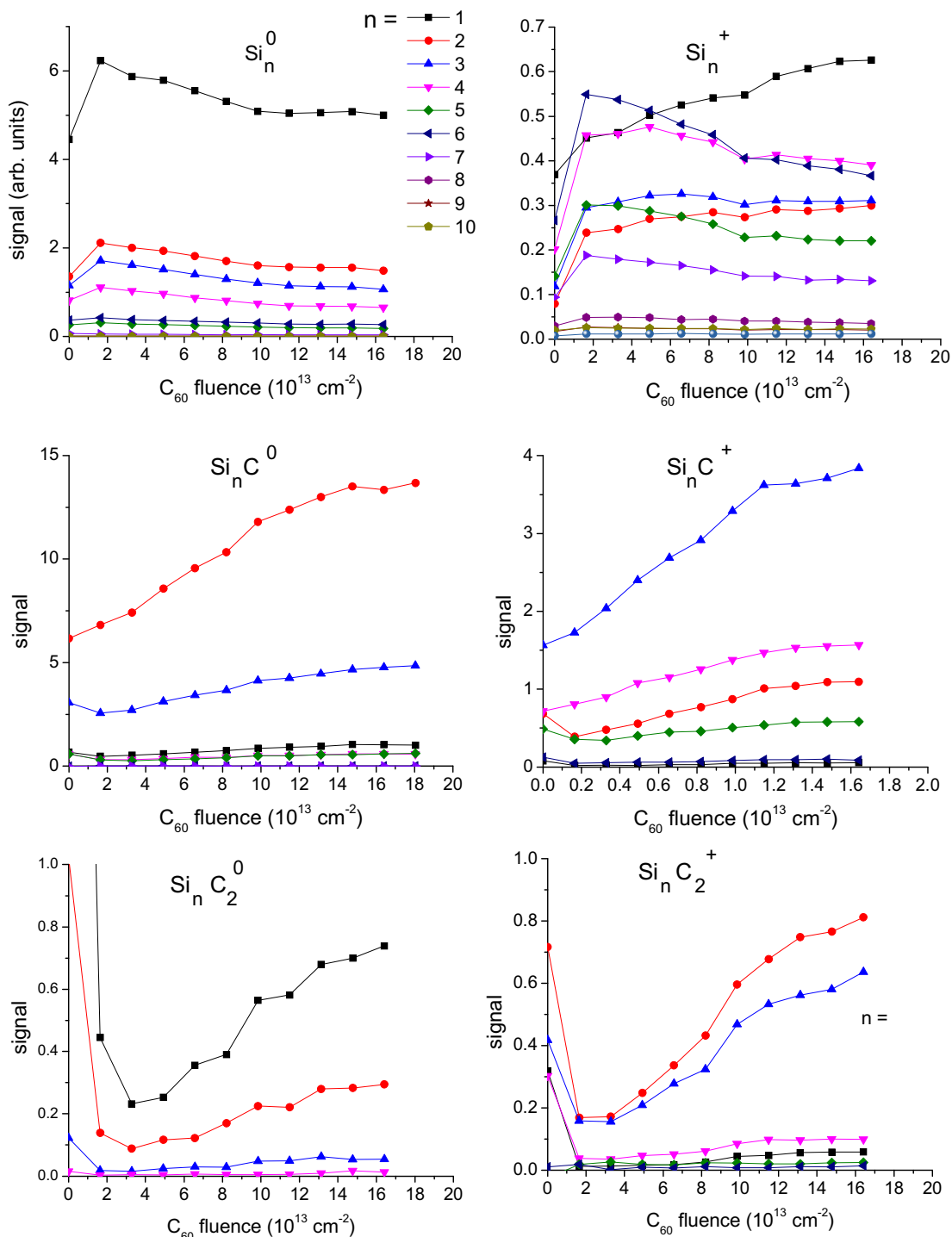


Fig. 2. Signal intensity of sputtered neutral and ionized  $\text{Si}_n\text{C}_m$  clusters vs. fluence of 40-keV  $\text{C}_{60}^+$  projectiles.

with increasing fluence. At the same time, all  $\text{Si}_n$  signals exhibit a strong increase which clearly indicates the removal of a contamination layer.

Looking at Fig. 2, it becomes obvious that the neutral and ionized clusters exhibit a qualitatively different behavior. The neutral yields reflect the trend which is to be expected upon carbon accumulation at the surface, i.e., the signals of bare  $\text{Si}_n$  clusters fall, while those of carbon containing clusters rise with accumulating  $\text{C}_{60}$  fluence. Some secondary ion signals, on the other hand, do not follow this expected trend. This is particularly obvious for the  $\text{Si}^+$  signal, which rises instead of falling with increasing  $\text{C}_{60}$  fluence. This finding reflects a typical matrix effect as is often observed in secondary ion mass spectrometry, i.e., a change of the secondary ion formation probability  $\alpha_x^+$  upon changes of the surface chemistry. Apparently, the presence of carbon at the surface enhances the value of  $\alpha_{\text{Si}^+}$  in a similar way as is well known for oxygen. A similar effect, although weaker, is also observed for the  $\text{Si}_2^+$  signal. Moreover, the ordering of the  $\text{Si}_n^+$  signals with respect to  $n$  is clearly different from that of the  $\text{Si}_n^0$  signals. While the neutral clusters exhibit a monotonous decrease with increasing  $n$ , the secondary ion signals largely overestimate the yields of larger clusters. This is due to the fact that the secondary ion formation probability increases with increasing cluster size, a phenomenon which has been observed before for many metal and semiconductor clusters [6].

The rise of  $\text{Si}_n\text{C}_m$  cluster yields with increasing  $\text{C}_{60}$  fluence is found to be more pronounced with increasing number  $m$  of carbon atoms in the cluster. This observation is in principle expected

considering the probability that an emitted silicon atom “finds”  $m$  carbon atoms in close proximity to form a cluster. In a purely statistical picture, one would assume the formation probability of an  $\text{Si}_n\text{C}_m$  cluster to scale with the surface concentrations of silicon and carbon as  $(c_{\text{Si}})^n \cdot (c_{\text{C}})^m$  [17]. However, other criteria such as the bonding configuration of the implanted C atoms must also play a role. If, for instance, each C atom implanted into the surface was bound to the same number of Si atoms and the carbon concentration was low enough to ensure that these bonding sites were all isolated from each other, one would assume the yield of  $\text{Si}_n\text{C}_m$  to vary roughly proportional to the surface carbon content (i.e.,  $c_{\text{C}}$ ). In the statistical case, the  $\text{Si}_n\text{C}_m$  yield observed for a fixed value of  $n$  should vary as the  $m$ -th power of that of  $\text{Si}_n\text{C}_1$ , while in the latter extreme all  $\text{Si}_n\text{C}_m$  should vary in the same way regardless of  $m$ . Looking at the measured signals, we find the yields to increase by factors of 2.0, 3.4 and 7.2 for  $m = 1, 2$  and 3, respectively, upon increasing the fluence from  $2$  to  $18 \times 10^{13} \text{ cm}^{-2}$ . These factors are in reasonable agreement with the statistical prediction, indicating that it is rather the total carbon concentration than the local bonding configuration which determines the yield.

At  $\text{C}_{60}$  fluences exceeding  $2 \times 10^{14} \text{ cm}^{-2}$ , the signals depicted in Fig. 2 do not change any further up to the maximum applied value of  $1.8 \times 10^{15} \text{ cm}^{-2}$ , indicating that steady-state sputter equilibrium conditions have been reached. The signal intensity distributions obtained under these conditions are shown in Fig. 3. Note that the  $\text{Si}^0$  signal was corrected for post-ionization probability, while all cluster signals are plotted directly as measured. Again, it is seen that secondary ions and neutrals exhibit a qualitatively different

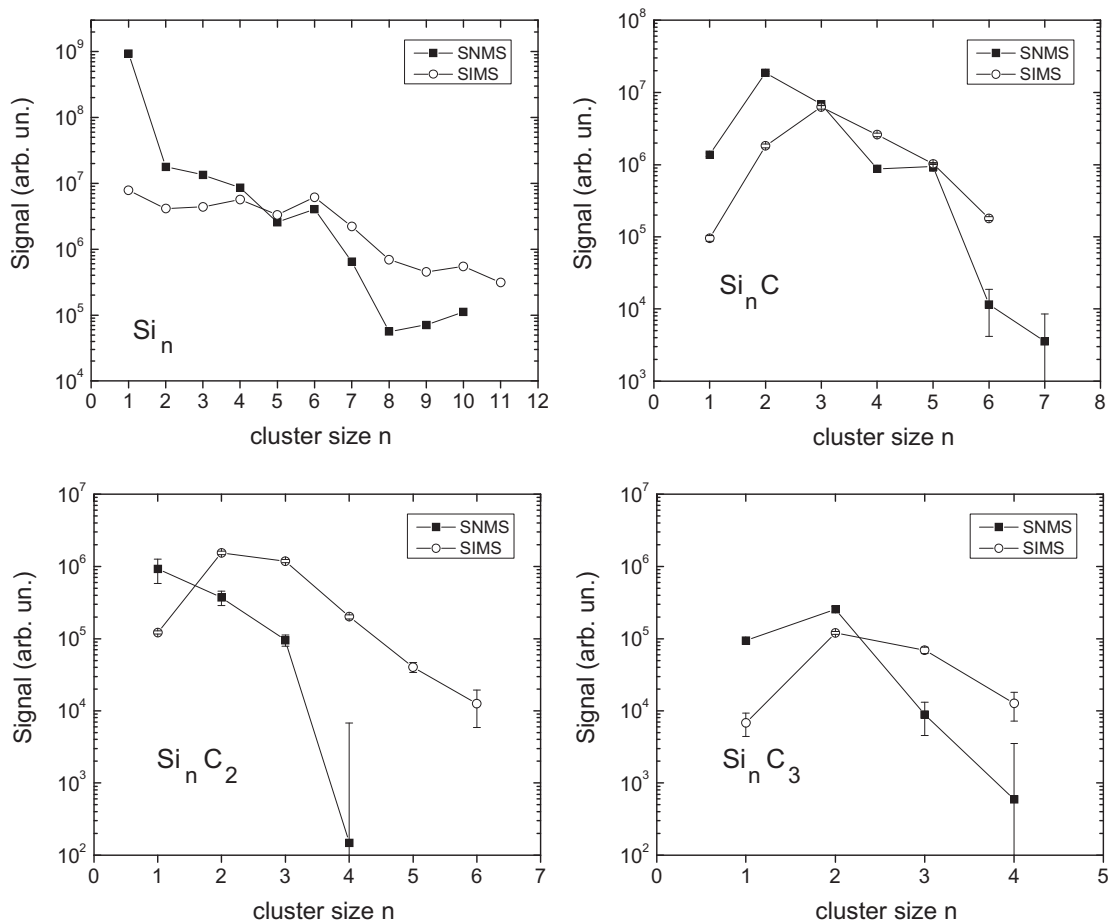


Fig. 3. Signal intensity of sputtered neutral and ionized  $\text{Si}_n\text{C}_m$  clusters under steady-state sputter equilibrium conditions reached at a  $\text{C}_{60}$  fluence exceeding  $2 \times 10^{14} \text{ cm}^{-2}$ . The measured  $\text{Si}^0$  signal was corrected for laser postionization efficiency estimated from ADK theory (see text).

behavior. The neutral  $\text{Si}_n$  yield falls significantly steeper with increasing  $n$  than that of the corresponding secondary ions, the signal distribution of which is virtually identical to those measured in Ref. [2]. Both data sets reflect a relative enhancement of the  $\text{Si}_6$  and  $\text{Si}_{10}$  yields, which is caused by the exceptional stability of these clusters. However, the neutral data clearly show that this does not make the cluster yields comparable to or even larger than that of the sputtered Si monomers. Moreover, the  $\text{Si}_n\text{C}$  and  $\text{Si}_n\text{C}_2$  yield distributions are found to peak at  $n = 2$  and 1 instead of 3 and 2 as suggested by the secondary ion data. In that respect, the interpretation of the secondary ion signals in terms of the relative cluster stabilities as given in Ref. [2] must be questioned.

Comparing our data to the MD simulations, it is important to note that the maximum  $\text{C}_{60}$  fluence reached in the simulations so far is about  $3.5 \times 10^{13} \text{ cm}^{-2}$ . We must therefore look at the yield distributions measured around that fluence. As a first result, our experimental data reveal that these distributions look virtually identical to those measured under steady-state conditions (Fig. 3). While the absolute values of the carbon containing clusters increase with increasing C accumulation at the surface, the relative distribution of the number of Si atoms combining with one, two or three C atoms does not change very much. In fact, due to the relatively small values of the surface carbon concentration, large variations are not expected even from the statistical cluster formation model, since  $c_{\text{Si}} \geq 0.9$  in all cases. One must therefore conclude that the distributions depicted in Fig. 3 must be largely determined by the relative cluster stability. The binding energies of  $\text{Si}_n\text{C}_m$  clusters [18] are listed in Table 1. It is evident that the bond energy of SiC is by far smaller than that of all other  $\text{Si}_n\text{C}_m$  clusters, while all  $\text{Si}_n\text{C}$  clusters with  $n > 1$  exhibit comparable binding energy per constituent atom. At the same time, the lowest dissociation threshold energies for these clusters are calculated as 5.5 eV (SiC), 7.5 eV ( $\text{Si}_2\text{C}$ ), 4.8 eV ( $\text{Si}_3\text{C}$ ) and 4.4 eV ( $\text{Si}_4\text{C}$ ), where the value for  $\text{Si}_3\text{C}$  refers to the most prominent fragmentation channel via  $\text{Si}_2\text{C}$  formation (all other possible channels have much higher threshold energies  $> 8$  eV) [18]. These data clearly suggest that  $\text{Si}_2\text{C}$  should be the most abundant sputtered cluster containing one carbon atom, and therefore renders the observed abundance distribution understandable.

Interestingly, this trend cannot be reproduced by the MD simulations, which predict SiC to be the most abundant sputtered cluster. At present, it is not clear whether this discrepancy is caused by the Tersoff potential, which was designed to describe a solid system and therefore may not permit a realistic description of small  $\text{Si}_n\text{C}_m$  molecules. In order to examine this possibility, it is necessary to calculate the equilibrium structures and binding energies of the clusters as predicted by this potential, which is beyond the scope of the present paper and will be the subject of a forthcoming publication.

The measured yield distributions can be connected with the carbon content of the bombarded surface. The total sputter yield, i.e., the total number of atoms (Si or C) ejected per single  $\text{C}_{60}$  impact is related to the partial yields  $Y(\text{Si}_n\text{C}_m)$  via

$$Y_{\text{tot}} = \sum_{n,m} (n + m) Y(\text{Si}_n\text{C}_m) = Y_{\text{Si}} + Y_{\text{C}} \quad (1)$$

**Table 1**  
Binding energies of  $\text{Si}_n\text{C}_m$  clusters (in eV/atom) as calculated from DFT (data taken from Ref. [18]).

Number of silicon atoms	Number of carbon atoms		
	1	2	3
1	2.72	5.14	5.47
2	4.35	5.09	5.75
3	4.46	5.08	5.48
4	4.44	5.27	5.35

**Table 2**

Relative partial sputter yields of neutral  $\text{Si}_n\text{C}_m$  clusters emitted from a silicon surface during 40-keV  $\text{C}_{60}^+$  bombardment under steady-state conditions. The data were normalized to the yield of sputtered neutral Si atoms.

Number of silicon atoms	Number of carbon atoms			
	0	1	2	3
0	0.16	–	–	–
1	1.0	0.015	0.010	0.0010
2	0.083	0.087	0.0017	0.0012
3	0.039	0.020	0.00027	0.00003
4	0.017	0.0018	–	–
5	0.0040	0.0015	–	–
6	0.0051	0.00001	–	–
7	0.00068	0.00000	–	–
8	0.00005	–	–	–
9	0.00005	–	–	–
10	0.00008	–	–	–

The quantities  $Y_{\text{Si}}$  and  $Y_{\text{C}}$  denote the total number of removed Si and C atoms (regardless of their bonding state) given by

$$Y_{\text{Si}} = \sum_n n \left[ \sum_m Y(\text{Si}_n\text{C}_m) \right] \quad \text{and} \quad Y_{\text{C}} = \sum_m m \left[ \sum_n Y(\text{Si}_n\text{C}_m) \right], \quad (2)$$

respectively. Under steady-state conditions, the ratio between these quantities must reflect the surface composition, yielding the equilibrium surface carbon concentration  $c_{\text{C}}$  as

$$c_{\text{C}} = \frac{Y_{\text{C}}}{Y_{\text{Si}} + Y_{\text{C}}} \quad (3)$$

In order to evaluate Eq. (3), the measured intensity distributions of Fig. 3 need to be corrected for the fact that our experiment detects the number density (and not the flux) of the sputtered species. This was done in the same way as described in detail elsewhere [5], i.e., by dividing the signal measured for a  $\text{Si}_n\text{C}_m$  cluster by  $n^{1.2}$ . The resulting yields, now normalized to that of sputtered Si atoms, are listed in Table 2. Since our experiment did not allow to measure the yields of neutral C atoms and bare  $\text{C}_m$  clusters, we first arbitrarily set these values to zero. Then, calculating the quantities in square brackets of Eq. (2) as column and row sums of Table 2 and inserting the resulting relative values of  $Y_{\text{C}}$  and  $Y_{\text{Si}}$  into Eq. (3), we find a steady-state atomic carbon concentration of 8.6%. This value can be compared to the prediction of the MD simulations. The carbon concentration profile calculated at a  $\text{C}_{60}$  fluence of  $3.5 \times 10^{13} \text{ cm}^{-2}$  is shown in Fig. 4. The data are presented as a function of depth or height measured with respect to the original silicon surface prior to the  $\text{C}_{60}$  bombardment. Note that this coordinate does not correspond to a true depth below the (fluence dependent) momentary surface, since the actual surface is heavily corrugated due to bombardment-induced topography evolution. In fact, analysis reveals that the height profile of the momentary surface at this fluence extends from 2.5 nm above to about 2.5 nm below the original silicon surface. Averaging the data of Fig. 4 over this range, we find a mean surface carbon concentration of 6.0%.

The data obtained here can be combined with the known sputter yield  $Y_{\text{Si}} = 200$  Si atoms/impact, which has been measured experimentally by eroding craters into a silicon surface under the same impact conditions as applied here [19]. Inserting this value into Eq. (3), we can calculate the absolute value of  $Y_{\text{C}}$  and find that 19 C atoms should in total be removed from the surface per  $\text{C}_{60}$  impact. At first sight, this value is surprising, since under steady-state conditions one would expect it to be equal to the number of atoms in the projectile. However, it is important to note that  $Y_{\text{C}}$  must equal the number of C atoms that are retained in the solid upon a projectile impact. Therefore, the data suggest that 41 projectile atoms must on average be backscattered from the surface under

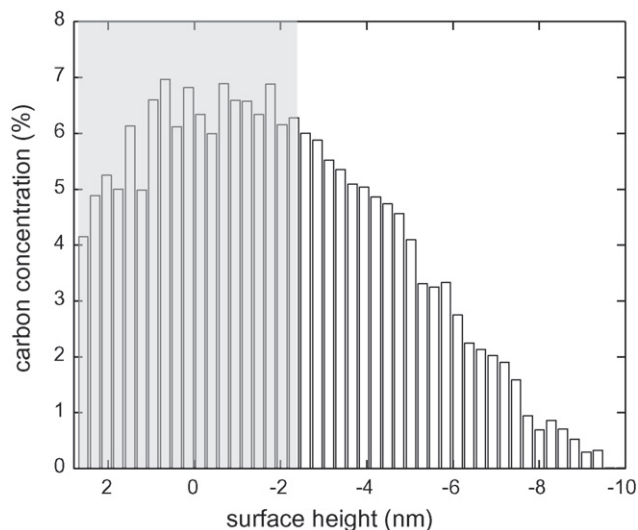


**Fig. 4.** Carbon concentration vs. height with respect to the original silicon surface as calculated from the MD simulations. The data were evaluated after 200 successive 20-keV  $C_{60}$  impacts onto a silicon surface, corresponding to a total projectile ion fluence of  $3.5 \times 10^{13} \text{ cm}^{-2}$ .

the bombarding conditions applied here. This finding contrasts the simulations, which predict about 39 projectile atoms to be retained in the solid for a 20-keV,  $45^\circ$  impact of  $C_{60}$  onto a fresh, undisturbed surface [20]. Moreover, the multi-impact simulations indicate that this value does not change significantly as a function of accumulated projectile fluence. This, in turn, predicts a value of  $Y_C = 39$  under steady-state conditions, which we can use to determine the missing contribution of carbon atoms sputtered in form of C or  $C_m$  to be 20 atoms/impact. This corresponds to 16% of the Si atom yield, which for simplicity was artificially introduced into Table 2 as a grey entry for the C atom yield (assuming that this additional contribution to  $Y_C$  solely arises from sputtered neutral C atoms). As a consequence, the equilibrium carbon surface concentration calculated from Eqs. (2) and (3) changes to 16%. Comparing this value to the MD prediction, it should be noted that the data of Fig. 4 was evaluated at a  $C_{60}$  fluence where steady-state conditions have not yet been established. From the measured increase of the  $Si_2C$  signal (which should to first order be proportional to the carbon surface concentration) in the fluence interval between  $3.5$  and  $18 \times 10^{13} \text{ cm}^{-2}$ , one would expect a further increase of  $c_C$  by roughly a factor 2 under steady-state conditions, which then renders the MD simulation to be in almost perfect agreement with the experimental data.

Besides the overall carbon concentration, the MD simulations also allow to determine the bonding configuration of the implanted carbon atoms. We find that under static conditions about 15% and 76% of the incorporated atoms have established bonds with three ( $sp^2$ -configuration) or four ( $sp^3$ -configuration) neighboring silicon atoms, respectively. With increasing  $C_{60}$  fluence, these fractions change only slightly to 19% and 74% at the highest simulated fluence. This finding is understandable, since the surface carbon concentration at the highest simulated fluence is still low enough to prevent significant interaction between implanted carbon atoms. It provides further support to the conclusion that it is not a change of the local bonding configuration but rather the statistical relation between the numbers of Si and C surface atoms which causes the fluence dependent changes of the cluster distributions observed in Fig. 2.

#### 4. Conclusions

In order to determine the composition distribution of sputtered clusters, it is essential to investigate the flux of sputtered neutral and ionized species rather than secondary ions alone. For the Si-C system investigated here, it is shown that the secondary ion formation probability of sputtered clusters may strongly depend on their nuclearity (i.e., the number of constituent atoms) and composition, rendering secondary ion mass spectral data misleading with respect to the true cluster yield distribution. The measured abundance distributions of  $Si_nC_m$  clusters ejected from a  $C_{60}$ -bombarded silicon surface can be understood in terms of the relative stabilities of these clusters. The variation of these distributions as a function of projectile ion fluence can be interpreted in terms of a simple statistical cluster formation model. The yield distributions measured under steady-state conditions can then be used to determine the equilibrium surface carbon content which is established by the balance between carbon implantation and re-sputtering induced by the  $C_{60}$  projectiles. The resulting surface carbon concentration appears to be in good agreement with the prediction of MD simulations.

#### Acknowledgments

We acknowledge support by the Deutsche Forschungsgemeinschaft in the frame of the Sonderforschungsbereich 616 “Energy dissipation at surfaces”. The authors thank Barbara Garrison, Mike Russo and Zbigniew Postawa for their contributions to the development of the scheme used for modeling multi-impact bombardment. We also thank Barbara Garrison for her intellectual contributions to this project as well as financial support for travel through her CHE-0901564 grant, which is administered by the Chemistry Division of the National Science Foundation. C. A. Briner acknowledges financial support in the form of a Summer Undergraduate Research with Faculty grant administered by the Undergraduate Center for Research and Creative Activities at the College of Charleston. Computational support for the MD simulations was provided by the Graduate Education and Research Services (GEARS) group of Academic Services and Emerging Technologies (ASET) at The Pennsylvania State University.

#### References

- [1] G. Gillen, J. Batteas, C.A. Michaels, P. Chi, J. Small, E. Windsor, A. Fahey, J. Verkouteren, K.J. Kim, *Appl. Surf. Sci.* 252 (2006) 6521.
- [2] I. Lyon, T. Henkel, D. Rost, *Appl. Surf. Sci.* 256 (2010) 6480.
- [3] K.D. Krantzman, B.J. Garrison, *J. Phys. Chem. C* 113 (2009) 3239.
- [4] M. Wahl, A. Wucher, *Nucl. Instrum. Methods B* 94 (1994) 36.
- [5] R. Heinrich, A. Wucher, *Nucl. Instrum. Methods B* 140 (1998) 27.
- [6] R. Heinrich, C. Staudt, M. Wahl, A. Wucher, *Secondary Ion Mass Spectrometry (SIMS XII)*, in: A. Benninghoven, P. Bertrand, H. N. Migeon, H.W. Werner (Eds.), Elsevier Science Amsterdam, 2000, 111.
- [7] A. Wucher, *IZV. An. SSSR Fiz.* 66 (2002) 499.
- [8] C. Staudt, A. Wucher, *Phys. Rev. B* 66 (2002) 075419.
- [9] K.D. Krantzman, A. Wucher, *J. Phys. Chem. C* 114 (2010) 5480.
- [10] R.M. Braun, P. Blenkinsopp, S.J. Mullock, C. Corlett, K.F. Willey, J.C. Vickerman, N. Winograd, *Rapid Commun. Mass Sp.* 12 (1998) 1246.
- [11] D. Willingham, D.A. Brenes, A. Wucher, N. Winograd, *J. Phys. Chem. C* 114 (2010) 5391.
- [12] A. Wucher, R. Heinrich, R.M. Braun, K.F. Willey, N. Winograd, *Rapid Commun. Mass Sp.* 12 (1998) 1241.
- [13] M.V. Ammosov, N.B. Delone, V.B. Krainov, *Sov. Phys. JETP* 64 (1986) 1191.
- [14] A. Benninghoven, *Surf. Sci.* 53 (1975) 596.
- [15] M.F. Russo, Z. Postawa, B.J. Garrison, *J. Phys. Chem. C* 113 (2009) 3270.
- [16] J. Tersoff, *Phys. Rev. B* 39 (1989) 5566.
- [17] H. Oechsner, *Springer Series in Chemical Physics*, Springer (1982) 106.
- [18] P. Pradhan, A.K. Ray, *J. Mol. Struct. – Theochem.* 716 (2005) 109.
- [19] J. Kozole, N. Winograd, *Appl. Surf. Sci.* 255 (2008) 886.
- [20] K.D. Krantzman, D.B. Kingsbury, B.J. Garrison, *Nucl. Instrum. Methods B* 255 (2007) 238.